

# PREDICTIONS OF CHIRAL RANDOM MATRIX THEORY AND LATTICE QCD RESULTS

T. WETTIG

*Institut für Theoretische Physik, Technische Universität München,  
D-85747 Garching, Germany*

Chiral random matrix theory makes very detailed predictions for the spectral correlations of the QCD Dirac operator, both in the bulk of the spectrum and near zero virtuality. These predictions have been successfully tested in lattice QCD simulations by several groups. Moreover, the domain of validity of random matrix theory has been predicted theoretically and identified in lattice data. In this talk, the current numerical evidence is reviewed.

## 1 Introduction

We are interested in learning as much as we can about the spectrum of the Euclidean QCD Dirac operator,  $\not{D} = \not{D} + ig\not{A}$ . One of the reasons for this interest is the Banks-Casher relation,  $\Sigma \equiv |\langle \bar{\psi}\psi \rangle| = \pi\rho(0)/V$ , which relates the chiral condensate to the spectral density,  $\rho(\lambda) = \langle \sum_n \delta(\lambda - \lambda_n) \rangle$ , of the Dirac operator at zero virtuality. Thus, the spontaneous breaking of chiral symmetry, a nonperturbative phenomenon with profound consequences for the hadron spectrum, is encoded in an accumulation of the small Dirac eigenvalues.

It has been realized that chiral random matrix theory (RMT) is a suitable tool to compute the distribution and the correlations of the small Dirac eigenvalues, see the talk by Verbaarschot in these proceedings and references therein. The first numerical evidence in support of this statement came from instanton liquid simulations.<sup>1</sup> The purpose of this talk is to verify the RMT-predictions by comparing them to lattice data. We shall see that the agreement between theory and numerical experiment is remarkable.

Recently, it has been shown<sup>2</sup> that the results obtained in RMT can also be derived directly from field theory (partially quenched chiral perturbation theory). Conceptually, this is a big step forward, while for actual calculations RMT seems to be the simpler alternative. It is comforting to know that the results of the two approaches agree with each other and with lattice data. Related topics are covered in the talks by Damgaard, Akemann, Papp, Markum, Stephanov, and Halasz (in order of appearance) in these proceedings.

## 2 Symmetries of the Dirac operator

Because of  $\{i\not{D}, \gamma_5\} = 0$ , the Dirac operator falls into one of three symmetry classes corresponding to the three chiral ensembles of RMT: chiral orthogonal (chOE), unitary (chUE), and symplectic (chSE) ensemble, respectively.<sup>3</sup> In most cases, the Dirac operator does not have additional symmetries and is described by the chUE. Exceptions are as follows ( $N_c$  = number of colors).

- continuum,  $N_c = 2$ , fermions in fundamental representation: chOE
- continuum, fermions in adjoint representation: chSE
- lattice,  $N_c = 2$ , staggered fermions in fundamental representation: chSE
- lattice, staggered fermions in adjoint representation: chOE

The overlap Dirac operator on the lattice has the symmetries of the continuum operator. There are a few exceptions where the Dirac operator does not have the usual chiral symmetries and is, therefore, described by the non-chiral RMT ensembles: QCD in three dimensions (UE), and the Wilson Dirac operator on the lattice (OE for  $N_c = 2$ , UE for  $N_c \geq 3$ , SE for the adjoint representation).

## 3 Correlations in the bulk of the spectrum

The full Dirac spectrum can be computed numerically using, e.g., a special version of the Lanczos algorithm. Which features of the spectrum are described by RMT in the bulk of the spectrum, i.e., away from the edges? The global spectral density is certainly not given by the RMT result since it is sensitive to the details of the dynamics. However, one can separate the average spectral density from the spectral fluctuations on the scale of the local mean level spacing. This process is called unfolding.<sup>4</sup> After unfolding, the spectral correlation functions are, up to a certain energy, given by RMT. This limiting energy is called the Thouless energy and will be addressed in Sec. 5.

The short- and long-range correlations of the eigenvalues are measured by quantities such as the distribution,  $P(s)$ , of spacings,  $s$ , between adjacent eigenvalues and the number variance,  $\Sigma^2(L) = \langle (n(L) - \langle n(L) \rangle)^2 \rangle$ , where  $n(L)$  is the number of eigenvalues in an interval of length  $L$ . In the bulk of the spectrum, the predictions of the chiral RMT ensembles for these quantities are identical to those of the corresponding non-chiral ensemble. They can be tested against lattice data. The predictions of RMT were confirmed with very high accuracy in the following cases: staggered fermions in  $SU(2)$ ,<sup>5,4</sup> in  $SU(3)$ ,<sup>6</sup> and in compact  $U(1)$ ,<sup>7</sup> respectively, Wilson fermions in  $SU(2)$ ,<sup>5</sup> and the overlap Dirac operator in  $SU(2)$ , in  $SU(3)$ , and in the adjoint representation of  $SU(2)$ , respectively.<sup>8</sup> Furthermore, the lattice data continue to agree with the RMT predictions in the deconfinement phase.<sup>6</sup> In all cases, the agreement was perfect, see  $P(s)$  in Fig. 1 for an example.

There is a very interesting question concerning staggered fermions: for  $N_c = 2$ , they have the symmetries of the chSE whereas the continuum symmetries are those of the chOE (and the other way around in the adjoint representation). While one should eventually see a transition from chSE to chOE behavior as the lattice spacing goes to zero, it is unlikely that this can be observed on present day lattices. The overlap Dirac operator, on the other hand, has the correct symmetries in all cases.

If a chemical potential is added to the problem, the Dirac eigenvalues are scattered in the complex plane. In this case,  $P(s)$  can also be constructed, see the talk by Markum.

#### 4 Correlations at the spectrum edge

Because the nonzero eigenvalues of  $i\cancel{D}$  come in pairs  $\pm\lambda_n$ , the Dirac spectrum has a “hard edge” at  $\lambda = 0$ . As mentioned in the introduction, the Dirac eigenvalues in this region are of great interest because of their connection to chiral symmetry breaking. The distribution of the smallest eigenvalues is encoded in the microscopic spectral density,  $\rho_s(z) = \lim_{V \rightarrow \infty} \rho(z/V\Sigma)/V\Sigma$ , which is universal and can be computed in RMT. One can also construct the distribution of the smallest eigenvalue,  $P(\lambda_{\min})$ , and higher-order spectral correlation functions. Analytical RMT results for these quantities are available. To compare these to lattice data, the only input one needs is the energy scale  $V\Sigma = \pi\rho(0)$ , which is obtained from the data by extracting  $\rho(0)$ .

The spectral correlations in the vicinity of  $\lambda = 0$ , in contrast to those in the bulk, are sensitive to the number of massless (or very light) quarks and to the topological charge  $\nu$ . This is another reason why the hard edge of the spectrum is more interesting than the bulk.

##### 4.1 Quenched approximation

The first evidence from the lattice for the universality of the microscopic spectral density came from an analysis by Verbaarschot of Columbia data for the valence quark mass dependence of the chiral condensate in SU(3) with staggered fermions.<sup>9</sup> Plotting all the data computed for various values of  $\beta = 6/g^2$  in a rescaled form suggested by RMT, it was observed that in the region of very small masses they all fell on the same universal curve given by RMT. The simulations were done with dynamical quarks, but the sea quarks were much heavier than the valence quark so that one effectively had  $N_f = 0$ .

The first direct lattice computation of the microscopic spectral quantities was done in quenched SU(2) with staggered fermions,<sup>10</sup> and the data were subsequently analyzed in more detail.<sup>11</sup> The agreement between lattice data

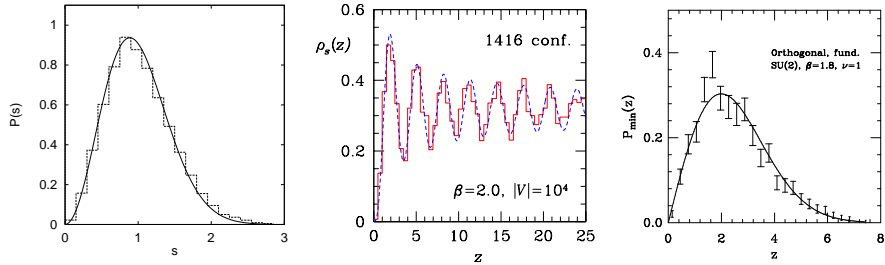


Figure 1. Spectral properties of the QCD lattice Dirac operator. The histograms represent lattice data, the curves are RMT predictions. Left: Nearest neighbor spacing distribution for SU(3), staggered fermions (chUE),  $V = 6^3 \times 4$ ,  $\beta = 5.0$ .<sup>6</sup> Middle: Microscopic spectral density for SU(2), staggered fermions (chSE),  $V = 10^4$ ,  $\beta = 2.0$ .<sup>10</sup> Right: Distribution of the smallest eigenvalue for SU(2), overlap Dirac operator (chOE),  $V = 4^4$ ,  $\beta = 1.8$ ,  $\nu = 1.8$ .

and RMT predictions was remarkably good, see  $\rho_s(z)$  in Fig. 1 for an example, but the analysis immediately raised a number of questions. First, why were the data consistent with the RMT predictions for topological charge  $\nu = 0$  even in weak coupling? Second, at what energies does RMT cease to be applicable? The answers will be given in Secs. 4.3 and 5.

Meanwhile, several groups have performed lattice simulations of the hard edge of the spectrum for almost all interesting cases: SU(3) with staggered fermions in three<sup>12</sup> and four<sup>13,14</sup> dimensions, the Schwinger model using both a fixed point and the Neuberger Dirac operator,<sup>15</sup> SU(2) and SU(3) with staggered fermions in the adjoint representation,<sup>16</sup> and the overlap Dirac operator in SU(2), in SU(3), and in the adjoint representation of SU(2), respectively.<sup>8</sup> The theoretical predictions of all three chiral ensembles (and of the UE) have thus been verified with high accuracy.

#### 4.2 Light dynamical fermions

In the chiral limit, the microscopic spectral correlations predicted by RMT depend on the number,  $N_f$ , of massless dynamical quarks. If the dynamical quarks are sufficiently heavy, the microscopic spectral correlations are given by the quenched result. There is an intermediate regime for quark masses of order  $1/V\Sigma$ , i.e., of the same order as the low-lying Dirac eigenvalues. In this “double-scaling” regime, the RMT results depend on the quark masses. So far, analytical results are only known for the chUE. Lattice simulations with very light dynamical quarks have been performed in SU(2) with staggered fermions,<sup>17</sup> corresponding to the chSE for which the corresponding RMT predictions were computed numerically. Again, very good agreement was found for  $\rho_s(z)$  and  $P(\lambda_{\min})$ .

### 4.3 Topology

Lattice simulations with staggered fermions show that the microscopic spectral quantities agree with the RMT predictions in the sector of zero topological charge, even in weak coupling. Presumably, the reason is that the would-be zero modes related to topology are shifted away from zero due to discretization errors of order  $a^2$ , where  $a$  is the lattice spacing. Thus, it is essential to use “better” Dirac operators which obey the Ginsparg-Wilson relation and for which the Atiyah-Singer index theorem holds. This has recently been done, in the Schwinger model using both a fixed point and the Neuberger Dirac operator,<sup>15</sup> and using the overlap Dirac operator in SU(2), in SU(3), and in the adjoint representation of SU(2), respectively.<sup>8</sup> (“Neuberger” and “overlap” refer to the same operator.) The lattice data agree very well with the RMT predictions also in sectors with  $\nu \neq 0$ , see  $P(\lambda_{\min})$  in Fig. 1.

## 5 Thouless energy

Since RMT predictions are derived without any knowledge of the details of the QCD dynamics, they are only valid up to a certain energy which is called the Thouless energy,  $E_c$ . To identify  $E_c$  for QCD, one needs two ingredients: (1) the fact that the random matrix model is applicable only if the kinetic terms in the chiral Lagrangian can be neglected, which is the case for  $L \ll 1/m_\pi$  (with  $L$  the linear extent of the four-volume and  $m_\pi$  the pion mass), and (2) the Gell-Mann–Oakes–Renner relation, connecting  $m_\pi$  to the quark mass and the chiral condensate. This gives rise to the theoretical prediction<sup>18,19</sup>  $E_c \sim f_\pi^2/\Sigma L^2$ , where  $f_\pi$  is the pion decay constant. This prediction was verified numerically in instanton liquid simulations<sup>18</sup> and in lattice simulations for SU(2)<sup>20,4</sup> and SU(3)<sup>14</sup> with staggered fermions. For lattice simulations, this roughly means that the domain of validity of the RMT approach is larger for larger lattice size and stronger coupling.

## 6 Summary

We now have a wealth of analytical and numerical evidence in support of the claim that the low-lying spectrum of the QCD Dirac operator is described by universal functions which can be computed, e.g., in RMT. This applies to the quenched approximation, to the full theory with dynamical quarks, and to trivial and nontrivial topological sectors. Moreover, we know the energy where the universality breaks down. Apart from a better analytical understanding of the Dirac spectrum, this also offers a variety of practical applications, such as better extrapolations to the thermodynamic limit,<sup>21</sup> the extraction of chiral

logarithms,<sup>22</sup> and perhaps the construction of hybrid Monte Carlo algorithms which would use the distribution of the small eigenvalues as input.

**Acknowledgments.** I thank the organizers for the invitation to this very stimulating workshop, and M.E. Berbenni-Bitsch, P.H. Damgaard, M. Göckeler, T. Guhr, H. Hehl, A.D. Jackson, J.-Z. Ma, H. Markum, S. Meyer, S. Nishigaki, R. Pullirsch, P.E.L. Rakow, A. Schäfer, B. Seif, J.J.M. Verbaarschot, H.A. Weidenmüller, and T. Wilke for very enjoyable collaborations.

## References

1. J.J.M. Verbaarschot, Nucl. Phys. B 427 (1994) 534.
2. J.C. Osborn, D. Toublan, and J.J.M. Verbaarschot, Nucl. Phys. B 540 (1999) 317.
3. J.J.M. Verbaarschot, Phys. Rev. Lett. 72 (1994) 2531.
4. T. Guhr et al., Phys. Rev. D 59 (1999) 054501.
5. M.A. Halasz and J.J.M. Verbaarschot, Phys. Rev. Lett. 74 (1995) 3920; M.A. Halasz, T. Kalkreuter, and J.J.M. Verbaarschot, Nucl. Phys. B (Proc. Suppl.) 53 (1997) 266.
6. R. Pullirsch et al., Phys. Lett. B 427 (1998) 119.
7. B.A. Berg, H. Markum, and R. Pullirsch, Phys. Rev. D 59 (1999) 097504.
8. R.G. Edwards et al., hep-th/9902117.
9. J.J.M. Verbaarschot, Phys. Lett. B 368 (1996) 137.
10. M.E. Berbenni-Bitsch et al., Phys. Rev. Lett. 80 (1998) 1146.
11. J.-Z. Ma, T. Guhr, and T. Wettig, Eur. Phys. J. A 2 (1998) 87, 425.
12. P.H. Damgaard et al., Phys. Lett. B 440 (1998) 129.
13. P.H. Damgaard, U.M. Heller, and A. Krasnitz, Phys. Lett. B 445 (1999) 366.
14. M. Göckeler et al., Phys. Rev. D 59 (1999) 094503.
15. F. Farchioni et al., hep-lat/9812018.
16. R.G. Edwards, U.M. Heller, and R. Narayanan, hep-lat/9902021.
17. M.E. Berbenni-Bitsch, S. Meyer, and T. Wettig, Phys. Rev. D 58 (1998) 071502.
18. J.C. Osborn and J.J.M. Verbaarschot, Phys. Rev. Lett. 81 (1998) 268, Nucl. Phys. B 525 (1998) 738;
19. R.A. Janik et al., Phys. Rev. Lett. 81 (1998) 264.
20. M.E. Berbenni-Bitsch et al., Phys. Lett. B 438 (1998) 14.
21. M.E. Berbenni-Bitsch et al., Nucl. Phys. B (Proc. Suppl.) 63A-C (1998) 820.
22. M.E. Berbenni-Bitsch et al., hep-lat/9901013.